The Crystal Structure of ReSe₂

N. W. ALCOCK* and A. KJEKSHUS

Kjemisk Institutt A, Universitetet i Oslo, Blindern, Oslo 3, Norway

The existence of one intermediate phase, the $ReSe_2$ phase, has been established in the rhenium-selenium system. The structure is triclinic with the lattice constants:

$a = 6.7272$Å, $b = 6.6065$Å, $c = 6.7196$Å
$\alpha = 118.93_7°$, $\beta = 91.82_6°$, $\gamma = 104.93_0°$

The pycnometric density is 9.237 g cm^{-3} at 25°C.
The space group is $P\bar{1}$ and the unit cell contains Re_I, Re_{II}, Se_I, Se_{II}, Se_{III}, and Se_{IV} in $(i) \pm (x,y,z)$:

Re_I with $x_1 = 0.4937$, $y_1 = 0.3038$, $z_1 = 0.3020$; $B_1 = 1.0$
Re_{II} with $x_2 = 0.4943$, $y_2 = 0.7474$, $z_2 = 0.3027$; $B_2 = 1.0$
Se_I with $x_3 = 0.2228$, $y_3 = 0.4875$, $z_3 = 0.3600$; $B_3 = 1.6$
Se_{II} with $x_4 = 0.2220$, $y_4 = 0.9830$, $z_4 = 0.3620$; $B_4 = 1.6$
Se_{III} with $x_5 = 0.7089$, $y_5 = 0.4893$, $z_5 = 0.1221$; $B_5 = 1.2$
Se_{IV} with $x_6 = 0.7089$, $y_6 = 0.9893$, $z_6 = 0.1221$; $B_6 = 1.2$

The $ReSe_2$ phase has diamagnetic susceptibility. Its structure is related to the $Cd(OH)_2$ type structure and it also shows similarities to rhenium cluster compounds.

A s far as we are aware, only one previous study[1] of the rhenium-selenium system has been published. Briscoe *et al.*[1] prepared a phase with composition Re_2Se_7 by wet chemical reaction. By thermal decomposition at 325—330°C in vacuum the same authors afterwards obtained a phase with composition $ReSe_2$.

As a link in continued studies of the properties of transition metal chalcogenides at this Institute it was considered of great interest to study the phase relationships in the rhenium-selenium system and to determine the crystal structures of possible phases.

EXPERIMENTAL

Materials. The rhenium metal used in this study was "Spectrographically standardized rhenium" from Johnson, Matthey & Co., Ltd. According to the supplied analysis it contained traces of Ag, Ca, Mg, and Cu. The highly purified selenium was a gift from Bolidens Gruvaktiebolag, Sweden. It carried the analysis (in ppm): Cu (2), Fe (0.8), K (0.3), Na (0.4), and non-volatile matter (12).

---

* Present address: University Chemical Laboratory, Cambridge, England.

Preparation. Samples with composition 50.00, 60.00, 66.67, 71.43, and 75.00 atomic % Se were made. The samples were prepared by heating the weighed quantities of rhenium and selenium in evacuated and sealed silica tubes. All samples were heated at 1000°C for 2 days, then cooled to 700°C, kept at this temperature for 20 days and finally cooled slowly to room-temperature over a period of 14 days.

X-Ray diffraction. All samples were crushed and X-ray photographs were taken in a Guinier camera of 80 mm diameter using strictly monochromatized $CuK\alpha_1$-radiation. For the calculation of lattice constants by the Guinier method, potassium chloride (Analar, The British Drug Houses Ltd., $a = 6.2919$ Å[2]) was added to the specimen as an internal standard. Lattice constants are expressed in Ångström units on the basis of $\lambda(CuK\alpha_1) = 1.54050$ Å.

X-Ray photographs were also taken with an integrating Weissenberg camera of 57.3 mm diameter using $CuK\alpha$-radiation. Intensity measurements were carried out microphotometrically using the multiple film technique. The intensities were corrected for absorption (see p. 83) and Lorentz and polarization factors. For calculation of F_c-values the atomic scattering factors were taken from Forsyth and Wells [4] or *International Tables.*[5] The agreement between F_0 and F_c is expressed by the reliability index $R = \Sigma||F_0| - |F_c||/\Sigma|F_0|$.

Density measurement. The density of $ReSe_2$ was determined pycnometrically at 25°C with kerosene as displacement liquid. To remove gases adsorbed by the sample the pycnometer was filled under vacuum with kerosene. The sample weighed approximately 2 g.

Magnetic susceptibility measurement. The magnetic susceptibility of $ReSe_2$ was measured by the Gouy method at three different maximum field strengths ($H_{max} = 4015, 4700,$ and 5110 Ø). The sample was filled in an evacuated and sealed Pyrex tube of 3 mm internal diameter to a height of 85 mm.

RESULTS

In the rhenium-selenium system only one intermediate phase is formed when the present method of preparation is used. The composition of this phase, estimated using the disappearing phase method on the Guinier photographs, is close to $ReSe_2$. Although the samples were cooled slowly, the Re_2Se_7 phase, which is reported[1] to decompose at 325—330°C, was not observed.

(i) *Unit cell and space group.* Since no unit cell of high symmetry could be found to fit all the lines on the complex Guinier photographs, *cf.* Table 1, single crystal work was started from the beginning. A large number of single crystals were present in the samples, of an extremely thin platy shape, generally rather longer in one direction than the other, with parallel sides and pointed terminations. They were very sensitive to deformation. Orientation of the crystals for oscillation and Weissenberg photographs was only possible using axes along or across the plates.

Examination of the photographs taken about the axis along the plates appeared to indicate monoclinic symmetry with the diad (*b'*) axis as rotation axis, but showed very curious extinctions. However, extensive attempts to refine the apparent cell constants with the aid of Guinier photograph data were quite unsuccessful. Eventually a careful inspection of Weissenberg photographs taken about the supposed *c'*-axis showed that the crystals might be treated as triclinic and indicated possible cell dimensions. Attempts to fit and refine these approximate dimensions by applying the method of least squares to the Guinier photograph data were successful. The de Wolff method [3] was used in a Fortran and SPS program written for the IBM 1620. The observed and calculated $\sin^2\Theta$ values, and the indices (in terms of the reduced

Table 1. Guinier photograph data of ReSe₂ taken with strictly monochromatized CuKα₁-radiation.

I_{obs}	sin²Θ × 10⁵ obs	sin²Θ × 10⁵ calc	hkl
st	1 460	1 454	100
w	1 780	1 776	001
vw	1 842	1 838	0$\bar{1}$1
w	2 637	2 635	10$\bar{1}$
vw	2 831	2 832	1$\bar{1}$1
vw	5 647	5 647	011
m	7 107	7 106	002
m	7 211	7 208	1$\bar{2}$0
vw	7 275		
m	7 353	7 353 / 7 369	0$\bar{2}$2 / 10$\bar{2}$
vw	8 162	8 162	2$\bar{1}\bar{1}$
vw	8 752	8 751	111
vw	8 786	8 782	201
st	9 460	9 459	2$\bar{2}$0
w	9 577		
vst	9 737	9 729 / 9 750	12$\bar{2}$ / 102
w	10 543	10 542	20$\bar{2}$
w	11 326	11 326	2$\bar{2}$2
w	11 425	11 431	120
vw	12 106	12 090	11$\bar{2}$
w	12 200	12 199	1$\bar{2}\bar{1}$
w	12 428	12 426	0$\bar{2}$3
w	12 640	12 643	1$\bar{3}$1
vw	12 885	12 881	012
vw	13 081	13 078 / 13 086	30$\bar{1}$ / 300
w	13 450	13 451	021
w	13 555	13 553	1$\bar{2}$3
vw	13 766	13 761 / 13 782	0$\bar{3}$1 / 3$\bar{1}$1
w	13 861	13 855	2$\bar{2}\bar{1}$
w	14 203	14 206 / 14 207	2$\bar{1}$2 / 12$\bar{3}$
w	14 436	14 424 / 14 433	1$\bar{1}$3 / 2$\bar{3}$1
vw	14 611	14 618	3$\bar{2}$0
vw	15 005	15 012	22$\bar{2}$
vw	15 297	15 302	202
m	15 660	15 657	10$\bar{3}$
m	15 990	15 985 / 15 988	1$\bar{3}$0 / 003
vw	16 543	16 545	0$\bar{3}$3
w	16 618	16 598 / 16 617 / 16 622	21$\bar{3}$ / 1$\bar{3}$3 / 30$\bar{2}$
vw	17 182	17 180	2$\bar{3}$0
vw	17 590	17 589 / 17 611	2$\bar{2}$3 / 121
vw	17 680	17 675 / 17 698	3$\bar{2}$2 / 030
w	17 901	17 904	220
w	18 235	18 234	20$\bar{3}$
vw	19 222	19 226 / 19 231	103 / 3$\bar{1}\bar{2}$
vw	19 592	19 597	2$\bar{3}\bar{3}$
st	20 739	20 743	1$\bar{2}\bar{2}$
vw	20 900		
st	21 055	21 052	0$\bar{2}$4
st	21 748	21 754	1$\bar{4}$2
w	22 252	22 238 / 22 282	12$\bar{4}$ / 11$\bar{3}$
vw	22 578	22 590	022
vw	22 746	22 771 / 22 775	0$\bar{1}$4 / 1$\bar{2}$4
w	22 882	22 880 / 22 901	13$\bar{1}$ / 11$\bar{4}$
vw	23 080	23 083	2$\bar{4}$2
w	23 264	23 259 / 23 264 / 23 266	4$\bar{1}$1 / 400 / 0$\bar{3}$4
vw	23 335	23 332	0$\bar{4}$2
vw	23 715	23 719	30$\bar{3}$
vw	23 765	23 761	302
vw	25 191	25 188	031
vw	26 913	26 931	4$\bar{2}$2
vw	28 429	28 423	004
vw	28 701	28 695 / 28 731	1$\bar{4}$0 / 4$\bar{3}$2
w	29 039	29 024 / 29 064	1$\bar{4}$4 / 4$\bar{1}$2
w	29 480	29 479	20$\bar{4}$
w	31 468	31 463	040
w	31 549	31 543	2$\bar{4}$4
vw	32 842	32 839	1$\bar{2}$3
w	33 215	33 231	0$\bar{2}$5
w	33 334	33 328 / 33 333 / 33 333	1$\bar{3}$2 / 32$\bar{4}$ / 2$\bar{3}$2
vw	33 821	33 822	12$\bar{5}$

Table 2. Lattice constants of the $ReSe_2$ phase. ($t = 20 \pm 2°C$).

Sample	Cell	a (Å)	b (Å)	c (Å)	α (°)	β (°)	γ(°)	V (Å³)
$ReSe_2$	R	6.7272	6.6065	6.7196	118.93_7	91.82_6	104.93_0	248.17
$ReSe$	R	6.7295	6.6070	6.7191	118.94_6	91.81_6	104.91_4	248.26
$ReSe_3$	R	6.7319	6.6077	6.7197	118.93_3	91.81_6	104.92_1	248.43
$ReSe_2$	M	26.0016	6.6065	11.7617	89.49_4	100.67_2	90.71_8	1985.34
$ReSe_2$	D	6.7272	6.6065	11.7617	89.49_4	100.43_5	104.93_0	496.34

Calculated standard deviation for $ReSe_2$:

$\Delta a = \pm 0.0008$ Å; $\Delta b = \pm 0.0006$ Å; $\Delta c = \pm 0.0005$ Å; $\Delta\alpha = \pm 0.006°$; $\Delta\beta = \pm 0.008°$; $\Delta\gamma = \pm 0.010°$; $\Delta V = \pm 0.04$Å³.

triclinic unit cell, **R**) are given in Table 1. The exceptionally good agreement between observed and calculated values leaves no doubt about the correctness of the indexing.

The lattice constants of $ReSe_2$ are listed in Table 2 together with the lattice constants of the $ReSe_2$ phase for the samples $ReSe$ and $ReSe_3$, which contain the $ReSe_2$ phase in equilibrium with Re and Se, respectively. The slight variations in the a-axes of the three samples indicate that the $ReSe_2$ phase has a narrow range of homogeneity.

The observed density of $ReSe_2$, 9.237 g cm⁻³, indicates that the unit cell contains 4 ($Z_c = 3.99$) $ReSe_2$-groups. The calculated density of $ReSe_2$ from the X-ray measurements is 9.211 g cm⁻³. The space group is $P\bar{1}$.

The apparent monoclinic symmetry is explicable on the basis of a pseudo monoclinic cell (**M**) containing 8 primitive cell volumes of **R** with $\alpha' = 89.49°$ and $\gamma' = 90.72°$. By considering the transformation matrix for axes and indices from **R** to **M**:

$$\begin{pmatrix} 4 & 1 & 0 \\ 0 & 1 & 0 \\ 0 & 1 & 2 \end{pmatrix}$$

the curious extinctions:

$h'0l'$ absent when $h' \neq 4n$ or $l' \neq 2n$,

observed for **M** can be explained. The lattice constants a', b', c', α', β', and γ' of **M** are listed in Table 2.

M has its b'-axis along the crystal plates and its c'-axis across the plates. For this reason the initial structural work (the [010]-projection) was carried out in relation to this cell. The results can also be expressed in terms of a doubly primitive cell (**D**) with the same b'- and c'-axes as **M**. The transformation matrix for axes and indices from **R** to **D** is

$$\begin{pmatrix} 1 & 0 & 0 \\ 0 & 1 & 0 \\ 0 & 1 & 2 \end{pmatrix}$$

The second part of the structural work was carried out in **D** (on its [001]-projection). The lattice constants a'', b'', c'', α'', β'', and γ'' of **D** have also been included in Table 2.

(ii) [010]-*Projection*. The relevant cells **R**, **M**, and **D** have a common b-axis and are accordingly identical in the [010]-projection.

This projection corresponds to rotation about the longer axis in the crystal plate, and the crystal was therefore easy to orient. Because of the shape of the crystals a correction for absorption was essential. It could be made fairly easily, as the large width/thickness ratio of the plates ($\sim$200) means that they can be treated as of infinite extent without serious error.

In this case the formula given in *International Tables* [6] shows that for a given plate thickness the correction depends only on the angles between the plate and the incident and diffracted X-ray beams, and a Fortran program was written for the IBM 1620, to apply the correction. The absorption corrections are sensitive to the plate's thickness, which is difficult to measure accurately, but unlike most corrections, show almost no correlation with $\sin^2\Theta$.

99 reflections were experimentally accessible, of which 4 had zero observed intensity, and 3 had unacceptably high absorption correction factors. At a late stage, 5 more with the highest observed intensities were excluded, suffering from extinction or observational errors (probably caused by film non-linearity), leaving 87 for refinement.

At this stage the crystals were believed to be monoclinic (in the monoclinic approximation of **M**). Attempts to derive trial structures by comparison with known structures, and from examination of a Patterson synthesis were unsuccessful, although not all the possible "monoclinic" space groups were tried. Direct methods for sign determination were then attempted, which rapidly gave probable signs of 50 of the strongest reflections. A Fourier projection evaluated with this set of signs showed the atomic positions clearly, indicating an apparent space group $P2/m$. Based on the atomic parameters deduced from this Fourier synthesis, structure factors were calculated giving $R = 0.24$ which was improved to 0.165 after two further Fourier syntheses. Least square refinement of coordinates and temperature factors gave an R-value of 0.104. (At this stage the assumed crystal thickness was changed from 0.0030 to 0.0019 mm which gave an improved R-factor of 0.094.)

Despite this fairly low R-value the difference synthesis still showed marked anomalies at the atomic positions, particularly those of the selenium atoms. The temperature factors of the non-identical selenium atoms were furthermore very different. These findings were attributed either to anisotropic thermal vibration or to the presence of a superlattice giving rise to two superimposed non-identical sets of atoms.

However, when it was discovered that the true symmetry of the crystal was $P\bar{1}$ rather than $P2/m$, it became clear that each apparent atom in the [010]-projection consisted of two atoms not related by symmetry, but almost completely overlapped. Stepwise refinement based on this knowledge gave a final R-value of 0.0894 corresponding to the following atomic parameters and B-values (relating to **R**, with coordinates $\pm(x,z)$):
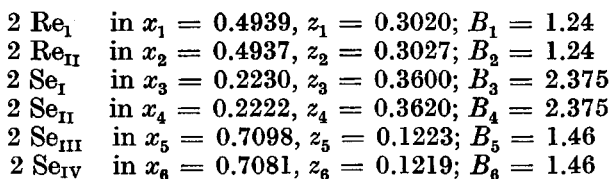
Table 3. Observed and calculated structure factors for $ReSe_2$. (Zone $h0l$ of R.)

hl	F_o	F_c	hl	F_o	F_c	hl	F_o	F_c
10	[185.6]^c	−295.7	12	[295.6]^c	367.9	44	[13.7]^a	10.6
20	46.4	60.8	22	152.1	−178.9	54	52.3	−33.9
30	180.7	−196.6	32	43.2	57.0	64	37.4	42.8
40	[221.0]^c	268.7	42	124.2	−123.7	$\bar{7}$5	66.8	65.5
50	165.3	−169.0	52	166.4	151.6	$\bar{6}$5	110.6	−146.1
60	107.7	105.1	62	111.0	−113.8	$\bar{5}$5	[252.7]^b	137.4
70	127.1	−94.1	72	73.4	91.3	$\bar{4}$5	90.7	−83.1
80	81.7	74.4	$\bar{8}$3	71.4	68.1	$\bar{3}$5	114.4	109.5
$\bar{8}$1	104.8	−105.2	$\bar{7}$3	138.4	−160.1	$\bar{2}$5	148.5	−149.1
$\bar{7}$1	94.8	94.8	$\bar{6}$3	147.0	150.9	$\bar{1}$5	154.9	146.2
$\bar{6}$1	[12.0]^a	3.1	$\bar{5}$3	73.5	−64.0	05	174.7	−165.3
$\bar{5}$1	25.5	25.9	$\bar{4}$3	96.8	106.3	15	156.9	152.5
$\bar{4}$1	168.5	−168.5	$\bar{3}$3	195.3	−215.2	25	72.4	−78.5
$\bar{3}$1	[332.6]^b	153.9	$\bar{2}$3	203.2	201.4	35	53.3	77.9
$\bar{2}$1	37.9	−40.2	$\bar{1}$3	176.2	−173.5	45	133.6	−140.4
$\bar{1}$1	69.2	73.1	03	180.2	184.0	55	91.3	119.2
01	80.8	−80.9	13	114.4	−113.9	$\bar{6}$6	33.7	32.7
11	32.4	34.2	23	87.9	92.8	$\bar{5}$6	34.0	−18.3
21	111.9	−121.8	33	186.5	−179.3	$\bar{4}$6	86.8	82.7
31	118.1	118.1	43	161.3	158.3	$\bar{3}$6	132.7	−120.7
41	37.0	34.4	53	27.1	−35.8	$\bar{2}$6	33.8	31.1
51	67.7	−54.4	63	15.1	20.0	$\bar{1}$6	23.9	24.2
61	68.8	−55.8	$\bar{7}$4	11.5	−13.5	06	56.8	56.9
71	68.4	60.6	$\bar{6}$4	23.2	31.3	16	113.2	−98.9
$\bar{8}$2	70.1	−59.5	$\bar{5}$4	[96.9]^{ab}	18.3	26	[84.0]^{ab}	33.1
$\bar{7}$2	72.8	73.6	$\bar{4}$4	50.4	−61.3	36	12.1	5.7
$\bar{6}$2	69.3	−63.6	$\bar{3}$4	53.8	−52.2	$\bar{4}$7	73.9	72.9
$\bar{5}$2	45.4	43.4	$\bar{2}$4	146.1	146.2	$\bar{3}$7	58.5	−51.7
$\bar{4}$2	[161.3]^b	−149.8	$\bar{1}$4	19.9	−14.0	$\bar{2}$7	44.1	56.1
$\bar{3}$2	[207.2]^c	279.8	04	98.7	−77.8	$\bar{1}$7	41.7	−56.2
$\bar{2}$2	134.9	−142.6	14	61.5	−53.8	07	74.4	66.5
$\bar{1}$2	28.0	−12.4	24	147.7	132.3	17	75.8	−96.2
02	[187.9]^c	−209.3	34	54.1	−54.4			

^{a} Unobserved reflection. The maximum possible value is listed.
^{b} High absorption correction applied.
^{c} Uncertain, due to extinction, or observational error.

$$2\ \text{Re}_I \quad \text{in } x_1 = 0.4939,\ z_1 = 0.3020;\ B_1 = 1.24$$
$$2\ \text{Re}_{II} \quad \text{in } x_2 = 0.4937,\ z_2 = 0.3027;\ B_2 = 1.24$$
$$2\ \text{Se}_I \quad \text{in } x_3 = 0.2230,\ z_3 = 0.3600;\ B_3 = 2.375$$
$$2\ \text{Se}_{II} \quad \text{in } x_4 = 0.2222,\ z_4 = 0.3620;\ B_4 = 2.375$$
$$2\ \text{Se}_{III} \quad \text{in } x_5 = 0.7098,\ z_5 = 0.1223;\ B_5 = 1.46$$
$$2\ \text{Se}_{IV} \quad \text{in } x_6 = 0.7081,\ z_6 = 0.1219;\ B_6 = 1.46$$

The B-values of overlapped atom pairs were kept equal, as it seemed unlikely that any apparent difference would be meaningful. The difference Fourier still showed the anomalies previously observed, but they were now less marked. Further attempts to remove them only led to increased R-values.

The observed and calculated structure factors are listed in Table 3, and the final Fourier map is shown in Fig. 1.
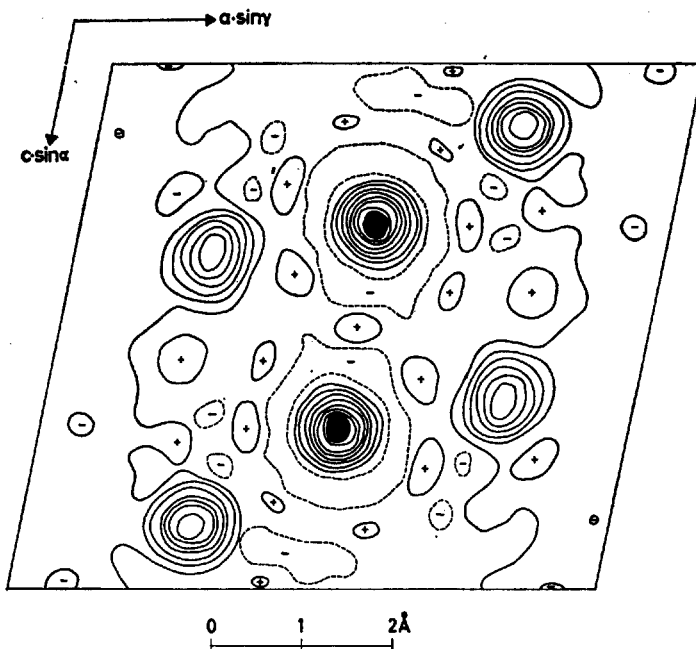
Fig. 1. Electron density projection of ReSe₂ along [010] (for R). Contours are at intervals of 10 e.Å⁻² generally, and at 20 e.Å⁻² around the rhenium atoms, which have filled centres. The zero contours are broken, and small elevations and depressions in the background are signed + and −, respectively.

(iii) [001]-*Projection of* **D**. Because of the fragility of the crystals, mounting them about the shorter axis of the plates was difficult; also many of the apparently single crystals examined proved to be very complex collections of crystals in disordered orientations. Eventually one was found which although multiple, appeared to have only one main component and satellites small enough not to be troublesome. This was mounted about the c-axis (referring to **D** or **M**). Examination of the Weissenberg photographs showed that most spots were doubled which was attributed to lineage structure in the crystal. However, this was not so severe as to prevent the measurement of integrated intensities including both components of each spot.

The intensities were converted to unitary structure factors after correction for Lorentz, polarization and absorption effects. With the aid of the known signs for the h00 reflections, application of inequalities and Sayre's relation gave signs for 29 out of 34 structure factors. A Fourier projection using this set of signs showed a plausible structure (with closely overlapped atoms), which was refined, mainly by the stepwise method, to $R = 0.096$.

All this work in the [001]-projection was performed in plane group *pmm*, under the assumption that the crystal was monoclinic. However, at this stage the correct triclinic cell was discovered, and it was realized that the doubling of the hk0 reflections, which had been attributed to lineage, was in fact caused

by the crystal being twinned with one set of reflections about twice as intense as the other.

Because it has been so difficult to find a suitable crystal an attempt was made to obtain satisfactory intensity data from the first crystal rather than to search for a better one. It did not prove very difficult to separate the contributions from each of the twins, as most spots consisted of two parts which could be indexed as $hk0$ of twin A and $h\bar{k}0$ of twin B. The average intensity ratio A:B was calculated and when the spots overlapped completely, the overall intensity could be divided proportionately. In all, 56 reflections were experimentally accessible, of which 12 were unobserved, 1 (common to the $h0l$ data) suffered from extinction, and 4 (removed at a later stage) were affected by high absorption (and possible indexing uncertainties), leaving 39 for refinement.

Table 4. Observed and calculated structure factors for ReSe$_2$. (Zone $hk0$ of **D**. The corresponding indices for **R** have been included. The F-values are scaled to correspond to four units of ReSe$_2$ per cell.)

$h''k''l''$	hkl	F_o	F_c	$h''k''l''$	hkl	F_o	F_c
100	100	[226.4]^c	−296.4	$\bar{4}40$	$\bar{4}4\bar{2}$	111.7	−110.4
200	200	53.0	58.9	$\bar{3}40$	$\bar{3}4\bar{2}$	[16.2]^a	7.1
300	300	190.9	−205.3	$\bar{2}40$	$\bar{2}4\bar{2}$	147.6	−155.2
400	400	273.1	288.3	$\bar{1}40$	$\bar{1}4\bar{2}$	312.2	304.5
500	500	186.4	−177.1	040	04$\bar{2}$	140.2	−148.8
600	600	119.8	113.0	140	14$\bar{2}$	[16.3]^a	8.6
700	700	122.7	−120.4	240	24$\bar{2}$	121.7	−116.8
800	800	97.9	92.3	340	34$\bar{2}$	[137.4]^b	191.5
$\bar{8}20$	$\bar{8}2\bar{1}$	[25.5]^a	6.8	440	44$\bar{2}$	118.0	−113.8
$\bar{7}20$	$\bar{7}2\bar{1}$	104.7	114.5	540	54$\bar{2}$	67.2	68.6
$\bar{6}20$	$\bar{6}2\bar{1}$	83.4	−84.1	640	64$\bar{2}$	62.4	−79.1
$\bar{5}20$	$\bar{5}2\bar{1}$	70.1	−63.3	$\bar{7}60$	$\bar{7}6\bar{3}$	44.3	−47.5
$\bar{4}20$	$\bar{4}2\bar{1}$	[166.3]^{ab}	36.8	$\bar{6}60$	$\bar{6}6\bar{3}$	46.0	−52.0
$\bar{3}20$	$\bar{3}2\bar{1}$	100.5	93.1	$\bar{5}60$	$\bar{5}6\bar{3}$	[45.0]^a	29.8
$\bar{2}20$	$\bar{2}2\bar{1}$	62.4	−57.6	$\bar{4}60$	$\bar{4}6\bar{3}$	56.5	50.6
$\bar{1}20$	$\bar{1}2\bar{1}$	13.0	−10.4	$\bar{3}60$	$\bar{3}6\bar{3}$	32.5	−28.3
020	02$\bar{1}$	13.1	−14.8	$\bar{2}60$	$\bar{2}6\bar{3}$	[18.8]^a	−6.2
120	12$\bar{1}$	46.2	−53.7	$\bar{1}60$	$\bar{1}6\bar{3}$	[18.8]^a	−8.1
220	22$\bar{1}$	77.6	86.9	060	06$\bar{3}$	32.5	−26.8
320	32$\bar{1}$	[167.6]^{ab}	41.6	160	16$\bar{3}$	59.6	45.0
420	42$\bar{1}$	73.0	−64.0	260	26$\bar{3}$	[44.4]^a	34.7
520	52$\bar{1}$	97.1	−83.7	360	36$\bar{3}$	56.0	−49.4
620	62$\bar{1}$	116.2	111.1	460	46$\bar{3}$	52.4	−50.3
720	72$\bar{1}$	[24.8]^a	9.3	$\bar{4}80$	$\bar{4}8\bar{4}$	[42.7]^{ab}	−56.4
$\bar{8}40$	$\bar{8}4\bar{2}$	80.7	−76.5	$\bar{3}80$	$\bar{3}8\bar{4}$	[116.8]^b	−22.0
$\bar{7}40$	$\bar{7}4\bar{2}$	61.0	66.3	$\bar{2}80$	$\bar{2}8\bar{4}$	76.7	97.3
$\bar{6}40$	$\bar{6}4\bar{2}$	103.3	−113.4	$\bar{1}80$	$\bar{1}8\bar{4}$	[64.7]^b	−15.4
$\bar{5}40$	$\bar{5}4\bar{2}$	[269.3]^b	189.4	080	08$\bar{4}$	[40.9]^{ab}	−55.5

^{a} Unobserved reflection. The maximum possible value is listed.
^{b} High absorption correction applied.
^{c} Uncertain, due to extinction.

Since the structure previously deduced from this projection was chemically completely acceptable (and, in fact, while allowing some variation, almost inescapable) it was taken as a trial structure. A set of structure factors calculated on this assumption gave $R = 0.187$. A stepwise refinement reduced the R-value rather slowly to 0.133, and removal of the 4 doubtful reflections and final refinement gave $R = 0.0755$. The final coordinates and B-values were (relating to **D**, with coordinates $\pm (x,y''; x,\frac{1}{2}+y'')$):

$$4 \text{ Re}_I \quad \text{in } x_1 = 0.4936, \, y_1'' = 0.1528; \, B_1 = 0.775$$
$$4 \text{ Re}_{II} \quad \text{in } x_2 = 0.4946, \, y_2'' = 0.0960; \, B_2 = 0.72$$
$$4 \text{ Se}_I \quad \text{in } x_3 = 0.2226, \, y_3'' = 0.3075; \, B_3 = 0.89$$
$$4 \text{ Se}_{II} \quad \text{in } x_4 = 0.2218, \, y_4'' = 0.3020; \, B_4 = 0.89$$
$$4 \text{ Se}_{III} \quad \text{in } x_5 = 0.7097, \, y_5'' = 0.4284; \, B_5 = 0.86$$
$$4 \text{ Se}_{IV} \quad \text{in } x_6 = 0.7080, \, y_6'' = 0.4280; \, B_6 = 0.86$$

The observed and calculated structure factors are listed in Table 4, and the final Fourier map is shown in Fig. 2. The coordinates, structure factors, and Fourier map are given for the full **D**-cell, although in projection its b''-
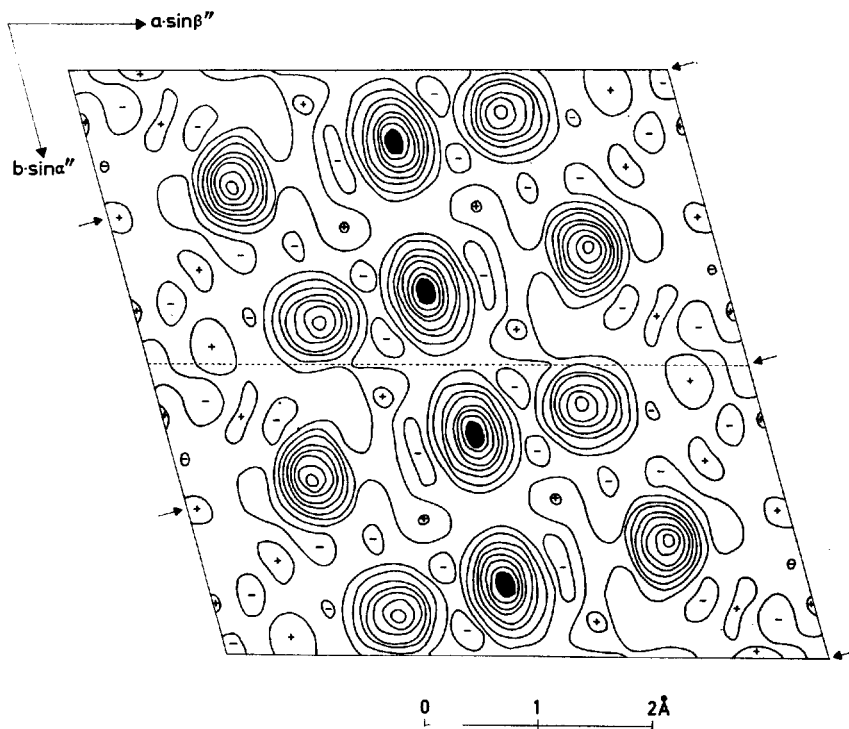
Fig. 2. Electron density projection of ReSe₂ along [001] (for **D**). Contours are at intervals of 10 e.Å⁻² generally, and at 20 e.Å⁻² around the rhenium atoms, which have filled centres. The background lies between 10 and 20 e.Å⁻² and small elevations and depressions are signed + and −, respectively. The arrows indicate the positions of the pseudo mirror planes, and the dotted line shows the repeating unit of the projection.

Table 5. Interatomic distances and angles in $ReSe_2$.

Interatomic distances (Å)

Re_I	— Re_I	: 2.64_6	Se_I	— Se_{II}	: 4.02_2	Se_{III}	— Se_I	: 3.35_7
	— Re_{II}	: 2.83_7		— Se_{II}	: 3.35_7		— Se_I	: 3.41_9
	— Re_{II}'	: 2.92_7		— Se_{III}	: 3.41_9		— Se_I	: 3.68_5
	— Re_{II}	: 3.68_0		— Se_{III}	: 3.68_5		— Se_I	: 3.76_5*
	— Se_I	: 2.38_2		— Se_{III}	: 3.76_5*		— Se_{II}	: 3.39_9
	— Se_I'	: 2.45_7		— Se_{IV}	: 3.40_4		— Se_{II}	: 3.42_8
	— Se_{II}	: 2.62_2		— Se_{IV}	: 3.42_1		— Se_{II}	: 3.72_9*
	— Se_{III}	: 2.38_5		— Se_{IV}	: 3.74_6*		— Se_{III}	: 3.27_9
	— Se_{IV}	: 2.60_4					— Se_{III}	: 4.29_0*
	— Se_{IV}'	: 2.66_5	Se_{II}	— Re_I	: 2.62_2		— Se_{IV}	: 3.27_9
				— Re_{II}	: 2.44_6		— Se_{IV}	: 3.30_3
Re_{II}	— Re_I	: 2.83_7		— Re_{II}'	: 2.61_8		— Se_{IV}	: 3.30_3
	— Re_I'	: 2.92_7		— Se_I	: 3.26_8			
	— Re_I	: 3.68_0		— Se_I	: 3.33_8	Se_{IV}	— Re_I	: 2.60_4
	— Re_{II}	: 3.07_7		— Se_I	: 4.02_2		— Re_I'	: 2.66_5
	— Se_I	: 2.34_5		— Se_{II}	: 3.56_5*		— Re_{II}	: 2.62_9
	— Se_{II}	: 2.44_6		— Se_{II}	: 4.02_6		— Se_I	: 3.40_4
	— Se_{II}'	: 2.61_8		— Se_{III}	: 3.39_9		— Se_I	: 3.42_1
	— Se_{III}	: 2.41_7		— Se_{III}	: 3.42_8		— Se_I	: 3.74_6*
	— Se_{III}'	: 2.60_6		— Se_{III}	: 3.72_9*		— Se_{II}	: 3.38_5
	— Se_{IV}	: 2.62_9		— Se_{IV}	: 3.38_5		— Se_{II}	: 3.39_2
				— Se_{IV}	: 3.39_2		— Se_{II}	: 3.69_6
Se_I	— Re_I	: 2.38_2		— Se_{IV}	: 3.69_6		— Se_{II}	: 3.78_2*
	— Re_I'	: 2.45_7		— Se_{IV}	: 3.78_2*		— Se_{III}	: 3.27_0
	— Re_{II}	: 2.34_5					— Se_{III}	: 3.30_3
	— Se_I	: 3.58_7*	Se_{III}	— Re_I	: 2.38_5		— Se_{III}	: 3.30_3
	— Se_I	: 4.05_2		— Re_{II}	: 2.41_7		— Se_{IV}	: 3.27_9
	— Se_{II}	: 3.26_8		— Re_{II}'	: 2.60_6		— Se_{IV}	: 4.29_0*
	— Se_{II}	: 3.33_8						

* Se—Se contacts between layers.

axis is halved. The pseudo mirror planes whose presence allowed considerable refinement in terms of plane group *pmm*, are indicated by arrows. The Fourier map shows that in this projection also, the atoms are overlapped, although the separations are a good deal larger in the *y*-direction than in either the *x*- or *z*-directions.

It is worth noting that both the projections examined were refined to unusually good *R*-values for this type of compound. This is almost certainly because the shape of the crystals allowed a very exact absorption correction to be made. On the other hand it will also be noticed that there are unexpectedly large differences between the *B*-values obtained in the two projections.

(iv) *The three-dimensional structure.* The determination of the correct *x,y,z* coordinate pairing depends on identifying the corresponding *x*-coordinates in each projection.

Superficially, the only real uncertainty seemed to be the correct pairing of coordinates for Re_I and Re_{II} where the refined *x*-parameters in the [001]-projection are somewhat different from those in the [010]-projection. A cross-check indicated the identification listed in section iii.

A more serious ambiguity, however, is due to halving of the *b″*-axis in the [001]-projection of **D**. The positions y, $\bar{y}$ and $\frac{1}{2}+y$, $\frac{1}{2}-y$ are equivalent

Table 5. Continued.

Interatomic angles (°)

Se$_I$	— Re$_I$	— Se$_I'$	: 113.7	Se$_{III}$	— Re$_{II}$	— Se$_{III}'$	: 81.4
		— Se$_{II}$	: 83.5			— Se$_{IV}$	: 81.7
		— Se$_{III}$	: 101.3	Se$_{III}'$	— Re$_{II}$	— Se$_{IV}$	: 77.3
		— Se$_{IV}$	: 86.0				
		— Se$_{IV}'$	: 162.3	Re$_I$	— Re$_I$	— Re$_{II}$	: 60.9
Se$_I'$	— Re$_I$	— Se$_{II}$	: 104.7			— Re$_{II}'$	: 64.4
		— Se$_{III}$	: 89.8	Re$_{II}$	— Re$_I$	— Re$_{II}'$	: 125.4
		— Se$_{IV}$	: 159.8				
		— Se$_{IV}'$	: 83.7	Re$_I$	— Re$_{II}$	— Re$_I'$	: 54.6
Se$_{II}$	— Re$_I$	— Se$_{III}$	: 161.5			— Re$_{II}$	: 76.9
		— Se$_{IV}$	: 80.8	Re$_I'$	— Re$_{II}$	— Re$_{II}$	: 131.5
		— Se$_{IV}'$	: 88.7				
Se$_{III}$	— Re$_I$	— Se$_{IV}$	: 81.8	Re$_I$	— Se$_I$	— Re$_I'$	: 66.3
		— Se$_{IV}'$	: 81.5			— Re$_{II}$	: 76.5
Se$_{IV}$	— Re$_I$	— Se$_{IV}'$	: 76.9	Re$_I'$	— Se$_I$	— Re$_{II}$	: 72.4
Se$_I$	— Re$_{II}$	— Se$_{II}$	: 114.2	Re$_I$	— Se$_{II}$	— Re$_{II}$	: 68.0
		— Se$_{II}'$	: 82.2			— Re$_{II}'$	: 89.3
		— Se$_{III}$	: 101.4	Re$_{II}$	— Se$_{II}$	— Re$_{II}'$	: 74.7
		— Se$_{III}'$	: 85.2				
		— Se$_{IV}$	: 161.7	Re$_I$	— Se$_{III}$	— Re$_{II}$	: 75.1
Se$_{II}$	— Re$_{II}$	— Se$_{II}'$	: 105.3			— Re$_{II}'$	: 103.3
		— Se$_{III}$	: 89.7	Re$_{II}$	— Se$_{III}$	— Re$_{II}'$	: 98.6
		— Se$_{III}'$	: 160.1				
		— Se$_{IV}$	: 83.8	Re$_I$	— Se$_{IV}$	— Re$_I'$	: 103.1
Se$_{II}'$	— Re$_{II}$	— Se$_{III}$	: 161.8			— Re$_{II}$	: 96.9
		— Se$_{III}'$	: 81.2	Re$_I'$	— Se$_{IV}$	— Re$_{II}$	: 88.0
		— Se$_{IV}$	: 89.6				

The primes added to some atoms are only for convenience in considering corresponding distances and angles.

in the full [001]-projection of **D**. For any pair of overlapped atoms two sets of three-dimensional coordinates can be formed with y-parameters y_k, $\bar{y}_k$; $\frac{1}{2} + y_l$, $\frac{1}{2} - y_l$ and $y_l, \bar{y}_l$; $\frac{1}{2} + y_k$, $\frac{1}{2} - y_k$ (combinations such as y_k, $\bar{y}_k$; y_l, $\bar{y}_l$ are sterically impossible). Both possibilities are equally valid. As one such coordinate pair can be arbitrarily chosen (in this case the Re$_I$, Re$_{II}$ coordinates) there are four possible combinations. However, the exchange of the Se$_{III}$ and Se$_{IV}$ coordinates produces a shift of only $\Delta y = 0.0006$ and may thus be neglected. (The mean x-, y-, and z-values for the two possibilities were accordingly taken for the final parameters.)

The intensities of the $hk1$ reflections were measured, and a comparison of F_o and F_c for the two possibilities indicated strongly that the correct combination for the Se$_I$ and Se$_{II}$ parameters is

$$\text{Se}_I \quad x_3 = 0.2226, \ y_3 = 0.4875$$
$$\text{Se}_{II} \quad x_4 = 0.2218, \ y_4 = 0.9830$$

rather than

$$\text{Se}_I \quad x_3 = 0.2226, \ y_3 = 0.9875$$
$$\text{Se}_{II} \quad x_4 = 0.2218, \ y_4 = 0.4830$$

The atomic arrangement is thus (with mean values of the x-parameters and B-values obtained in the two projections) in terms of space group $P\bar{1}$ (cell **R**):

Re_I, Re_II, Se_I, Se_II, Se_III, and Se_IV in (i) $\pm$ (x,y,z)

Re_I with $x_1 = 0.4937$, $y_1 = 0.3038$, $z_1 = 0.3020$; $B_1 = 1.0$

Re_II with $x_2 = 0.4943$, $y_2 = 0.7474$, $z_2 = 0.3027$; $B_2 = 1.0$

Se_I with $x_3 = 0.2228$, $y_3 = 0.4875$, $z_3 = 0.3600$; $B_3 = 1.6$

Se_II with $x_4 = 0.2220$, $y_4 = 0.9830$, $z_4 = 0.3620$; $B_4 = 1.6$

Se_III with $x_5 = 0.7089$, $y_5 = 0.4893$, $z_5 = 0.1221$; $B_5 = 1.2$

Se_IV with $x_6 = 0.7089$, $y_6 = 0.9893$, $z_6 = 0.1221$; $B_6 = 1.2$

Despite the low values of R in these projections the three-dimensional coordinates cannot be considered to be determined with such accuracy. Particularly it should be remembered that no allowance has been made for anisotropic thermal vibration, which can be simulated accurately by half atoms with small separation [7] and accordingly in projection cannot be distinguished from overlapped atoms. Taking all error factors into consideration, it is likely that the interatomic distances listed in Table 5 have estimated standard deviations of about 0.02 Å, or overall error limits of about ±0.05 Å.

(v) *Interatomic distances and coordination.* The coordination around the rhenium and selenium atoms can be seen from Fig. 3. Interatomic distances and angles are listed in Table 5.

Each rhenium atom (Re_I and Re_II have nearly the same configuration of near neighbours) is surrounded by six selenium atoms at the corners of a somewhat distorted octahedron. The rhenium atom is shifted towards one face of its octahedron giving three shorter and three longer Re—Se distances, and three significantly short Re—Re distances, directed approximately through edges of the octahedron. This may be seen from Fig. 3 and the section through the plane containing the rhenium atoms shown in Fig. 4.

Each selenium atom is coordinated to three rhenium atoms at the base of a pyramid with the selenium atom at the top. All the four possible arrange-
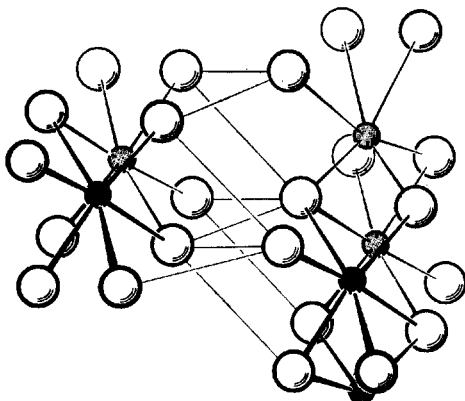

Fig. 3. The ReSe_2-structure. The smaller circles represent the rhenium atoms and the larger circles the selenium atoms.
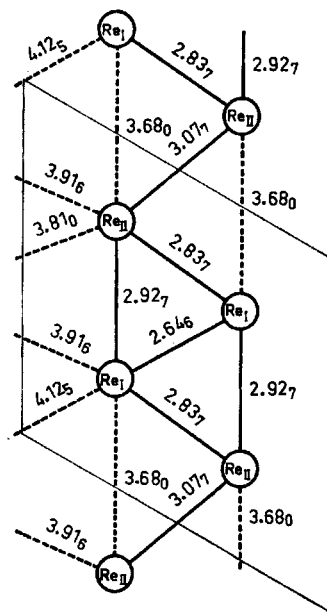
Fig. 4. Section through the plane containing the rhenium atoms. (This plane is approximately parallel to the (100)-plane.)

ments of short and long distances occur. The selenium atoms are surrounded by twelve selenium atoms at the corners of a distorted cuboctahedron.

An alternative description of the $ReSe_2$ structure is in terms of the pseudo hexagonal close-packed arrangement of the selenium atoms. The rhenium atoms occupy half of the octahedral interstices in the close-packed selenium array, every alternate layer of holes being completely filled. The stacking sequence of the selenium atoms is $|AB|CA|BC|$ with the layers parallel to (100).

As can be seen from Fig. 3, $ReSe_2$ has a pronounced layer structure with only long Se—Se contacts between the layers. This causes the platy habit of the crystals and their easy deformation. It is well known from studies of similar layer structures (see e.g. Mitchell [8] and Jellinek [9]) that polymorphism with a changed sequence may occur, produced by dislocations. A superstructure with a multiple a-axis of that reported here may well also occur for $ReSe_2$. Indeed a few spots attributable to crystals with a doubled a-axis were noticed on some of the Weissenberg photographs, and the unindexed lines on the Guinier photographs, cf. Table 1, may also be caused by such crystals.

The pronounced layer structure also gives the possibility of extra atoms being inserted between the layers. It is worth noting that the ReSe and $ReSe_3$ samples both have a slightly longer a-axis (and a correspondingly larger volume) than the sample with composition $ReSe_2$, cf. Table 2. This expansion may indicate that a few atoms are intercalated in the lattice when $ReSe_2$ is in equilibrium with rhenium or selenium.

The $ReSe_2$ structure is closely related to the $Cd(OH)_2$ type structure. Indeed this relationship is so close that one may well ask: Why does $ReSe_2$ adopt a triclinic structure instead of the more highly symmetrical trigonal

Cd(OH)$_2$ type structure. By comparison with compounds having the Cd(OH)$_2$ type structure (see *e.g.* Kjekshus and Pearson [10]) it is evident that the distortion cannot be due to a simple geometrical reason resulting from the relative size of the rhenium and selenium atoms, as *e.g.* HfS$_2$ has the regular Cd(OH)$_2$ type structure. Neither can it be attributed to a Jahn-Teller distortion as all the outer electrons of the rhenium atoms are involved in bond formation (see below). In the ReSe$_2$ structure the largest distortion is not a deformation of the symmetry of the selenium layers, but a shift of the rhenium atoms from the centres of the selenium octahedra. The short Re—Re distances observed (*cf.* Table 5 and Fig. 4) indicate that bonds exist between the rhenium atoms, and the primary cause of the distortion is probably the formation of these bonds with the associated movement of the rhenium atoms towards each other.

The effect of these Re—Re bonds on the outer electron configuration of the rhenium atoms can be studied by the general (8—N) rule:[11-14]

$$(n_e + b_a - b_c)/n_a = 8$$

where n_e is the total number of valence electrons (excluding any unshared electrons on the cations); n_a is the number of anions; b_a is the number of electrons involved in forming anion-anion bonds; b_c is the number of electrons involved in forming cation-cation bonds, all these values being calculated per formula unit of the compound. (This rule is a mathematical formulation of the need for all the anions in the crystal to have a complete octet [14].)

In ReSe$_2$ there are no localized unpaired *d*-electrons on the rhenium atoms (see section vi) and so their contribution to n_e must be either 7, 5, 3, or 1 electron. Each selenium atom contributes 6 electrons, so:

$n_e = 19, 17, 15,$ or 13;
$n_a = 2;$
$b_a = 0$ (from the crystal structure);

and therefore

$b_c = 3, 1, -1,$ or $-3,$ respectively.

The last two figures are physically meaningless and so each rhenium atom must on average use either 3 or 1 electron in forming Re—Re bonds, *i.e.* in the whole cell with 4 ReSe$_2$ units, there must be 6 or 2 Re—Re two-electron bonds. Examination of the crystal structure (*cf.* Fig. 4 and Table 5) shows that in each cell there is one short Re—Re distance (2.64$_6$ Å), less than those found in h.c.p. rhenium metal (2.740 Å (6) and 2.760 Å (6) according to Swanson and Fuyat [15] and Sims *et al.*[16]) four relatively short distances (2.83$_7$ Å (2) and 2.92$_7$ Å (2)) and one longer, but still significantly short distance (3.07$_7$Å (2 × 1/2). In no way can two bonds be chosen from this set. Thus the (8—N) rule can only be satisfied by assuming that all these six close approaches are two-electron bonds, and that the rhenium atoms use all their outer electrons in bonding. (Minor errors in the rhenium atomic positions will not affect the number of bonds; and allowing the selenium atoms to have an outer shell of 10 electrons requires 2 Se—Se bonds per cell, in disagreement with the observed crystal structure.)

The groups of rhenium atoms bound together in ReSe₂ may be compared with the rhenium clusters in $[Re_3Cl_{12}]^{3-}$, Re_3Cl_9 and similar compounds.[17],[18] These compounds have groups of three rhenium atoms arranged in equilateral triangles, with very short Re—Re distances of 2.48 Å. The rhenium atoms in ReSe₂ are also grouped in triangles (sharing alternate edges and corners), which suggest that the metal atom orbitals involved may be similar in each case. The bonds in ReSe₂ are much longer, and they compare more closely with the Ta—Ta distance of 2.90 Å reported [19] in $[Ta_6Cl_{12}]^{2+}$. (The shortest Re—Re distances in the metal are 2.740 and 2.760 Å; the corresponding Ta—Ta distances in metallic tantalum [20] are 2.863 Å.) The resemblance between ReSe₂ and the Re₃ clusters in the chloro-compounds seems close enough to allow ReSe₂ to be classified as a cluster compound; the differences in the rhenium clusters may well be attributed to the differing numbers of electrons available: 6 electron-pairs to 3 rhenium atoms in $[Re_3Cl_{12}]^{3-}$ and 6 electron-pairs to 4 rhenium atoms in ReSe₂.

Corresponding to the distorted $Cd(OH)_2$ type structure of ReSe₂, distorted rutile, pyrite, and marcasite type structures also occur, which can be explained on the basis of metal-metal bond formation from the general (8—N) rule.[21] Changes in the interactions in relation to the number of d-electrons, their degeneracy, critical metal-metal separation, etc. give variations in the observed metal-metal distances similar to those observed in ReSe₂. The length of the bonds also depends on the indirect metal-metalloid-metal interaction as well as the direct metal-metal interaction (cf. Goodenough [22]) and it is therefore difficult to discuss the significance of the Re—Re bond lengths.

ReSe₂ is the only known example of a distorted $Cd(OH)_2$ type structure among similar compounds and the reason for the lack of metal-metal bonds and corresponding lack of distortion in the other compounds of the transition metals must be considered. In TiS_2, $TiSe_2$, $TiTe_2$, ZrS_2, $ZrSe_2$, $ZrTe_2$, HfS_2, and $HfSe_2$ (cf. Ref. 10), the general (8—N) rule readily explains this, while with $NiTe_2$, $PdTe_2$, PtS_2, $PtSe_2$, and $PtTe_2$ (cf. Ref. 10) the reasonable assumption of a non-bonding t_{2g}^6 configuration on the metal atoms can be made. In the 1s-modifications of TaS_2 (Jellinek [9]) and $TaSe_2$ (Bjerkelund and Kjekshus [23]) and $RhTe_2$ and $IrTe_2$ (cf. Ref. 10) information on the electric and magnetic properties, required for application of the (8—N) rule is lacking.

(vi) *Magnetic properties*. The magnetic susceptibility of ReSe₂ was measured at temperatures between 90 and 725°K. The susceptibility is, as shown in Fig. 5, numerically slightly smaller than the expected diamagnetism resulting from
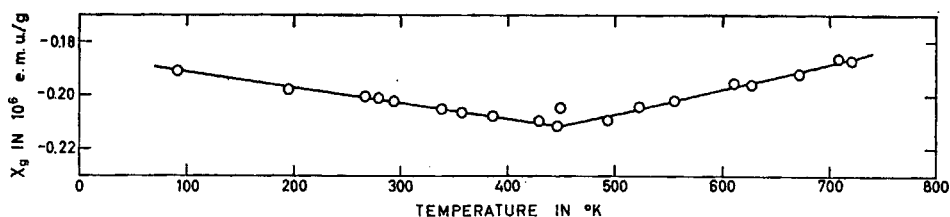

Fig. 5. The magnetic susceptibility of ReSe₂ as a function of temperature.

the atomic cores. The core contribution is -0.36×10^{-6} e.m.u. per gram $ReSe_2$ calculated from the diamagnetic corrections -28×10^{-6} e.m.u. per mole Re^{4+} (Klemm [24]) and -47.6×10^{-6} e.m.u. per mole Se^{2-} (Angus [25]). By subtracting this value from the measured susceptibility the total susceptibility of localized, non-bonding electrons, valence electrons, and conduction electrons is obtained. The temperature independent, exceedingly low susceptibility suggests very strongly that no unpaired d-electrons are present on the rhenium atoms.

REFERENCES

1. Briscoe, H. V. A., Robinson, P. L. and Stoddart, E. M. *J. Chem. Soc.* **1931** 1439.
2. Hambling, P. G. *Acta Cryst.* **6** (1953) 98.
3. de Wolff, P. M. *Advan. X-Ray Anal.* **6** (1962) 1.
4. Forsyth, J. B. and Wells, M. *Acta Cryst.* **12** (1959) 412.
5. *International Tables for X-Ray Crystallography.* The Kynoch Press, Birmingham 1962, Vol. III, p. 210.
6. *International Tables for X-Ray Crystallography.* The Kynoch Press, Birmingham 1959, Vol. II, p. 306.
7. Kartha, G. and Ahmed, F. R. *Acta Cryst.* **13** (1960) 532.
8. Mitchell, R. S. *Z. Krist.* **108** (1956) 296, 341.
9. Jellinek, F. *J. Less-Common Metals* **4** (1962) 9.
10. Kjekshus, A. and Pearson, W. B. *Progr. Solid State Chem.* **1** (1964) 83.
11. Mooser, E. and Pearson, W. B. *Progr. Semiconductors* **5** (1960) 103.
12. Hulliger, F. and Mooser, E. *J. Phys. Chem. Solids* **24** (1963) 283.
13. Pearson, W. B. *Acta Cryst.* **17** (1964) 1.
14. Kjekshus, A. *Acta Chem. Scand.* **18** (1964) 2379.
15. Swanson, H. E. and Fuyat, R. K. *Natl. Bur. Std. (U.S.) Circ.* 539 II (1953), p. 13.
16. Sims, C. T., Graighead, C. M. and Jaffee, R. I. *J. Metals* **7** (1955) 168.
17. Bertrand, J. A., Cotton, F. A. and Dollase, W. A. *Inorg. Chem.* **2** (1963) 1166.
18. Cotton, F. A. and Mague, J. T. *Proc. Chem. Soc.* **1964** 233.
19. Vaughan, P. A., Sturdivant, J. H. and Pauling, L. *J. Am. Chem. Soc.* **72** (1950) 5477.
20. Swanson, H. E. and Tatge, E. *Natl. Bur. Std. (U.S.) Circ.* 539 I (1953), p. 29.
21. Kjekshus, A. *To be published.*
22. Goodenough, J. B. *Magnetism and the Chemical Bond,* John Wiley & Sons, New York —London 1963.
23. Bjerkelund, E. and Kjekshus, A. *To be published.*
24. Klemm, W. *Z. anorg. allgem. Chem.* **246** (1941) 347.
25. Angus, W. R. *Proc. Roy. Soc. (London)* **A 136** (1932) 569.